



## A mechanics-induced complication of impression creep and its solution: application to Sn–3.5Ag solder

Deng Pan, I. Dutta\*

*Department of Mechanical Engineering, Center for Materials Science and Engineering, Naval Postgraduate School, Monterey, CA 93943, USA*

Received 31 July 2003; received in revised form 8 January 2004

### Abstract

Impression creep, wherein a flat-tipped cylindrical punch is used to load a small area of the specimen in nominally uniaxial compression, enables testing of very small material volumes and miniaturized components with minimal sample preparation. One of the attractive features of the impression creep test is its ability to establish steady-state within very short times for rapidly creeping materials. However, for relatively slowly creeping materials, a considerable time is necessary for the evolution of a steady-state plastic zone under the punch, resulting in a prolonged period of decreasing creep rate even when the constitutive creep behavior is strain-independent. This test-dependent transient behavior, where the creep rate decreases slowly even at very long test times, complicates the determination of true material creep parameters. Here, we discuss the source of this problem, and prescribe a methodology to substantially shorten the required test times in order to make the test technologically attractive. Because of the emerging importance of lead-free solders in microelectronics packaging, the analysis presented here is based on finite element simulations of eutectic Sn–3.5Ag solder, deforming via power-law creep.

© 2004 Published by Elsevier B.V.

*Keywords:* Impression creep; Lead-free solder; Finite element model; Sn–3.5Ag

### 1. Introduction

Impression creep, which uses a cylindrical punch with a flat end to load a small area of the specimen under minimal uniaxial compression, has been used extensively to characterize the creep properties of materials [1–16]. Because it enables probing very small material volume, it is particularly attractive for testing of modern micro-components such as parts of microelectronic packages or MEMS devices. It has been shown that the stress and the temperature dependencies obtained from impression creep tests display good agreement with the results of conventional creep tests [1,17,18]. A steady-state creep region is established at a constant punch stress after a transient period, e.g., primary creep, and unlike conventional creep, no tertiary creep stage ensues thereafter. Under power law creep, it is found that the impression velocity and the punch stress conform to the same power law as that for the conventional creep [1,16,19]. From the impression velocity ( $V$ ) versus punch stress ( $\sigma_p$ ) data, the creep

strain rate versus effective creep stress relationship may be provided by using appropriate conversion factors [18,20], which vary with material properties [1].

One of the attractive features of the impression creep test is its ability to establish steady-state creep within very short times for rapidly creeping materials. The resulting stress exponent,  $n$ , as well as the activation energy,  $Q$ , are comparable to those obtained from uniaxial tests, e.g., [2,3,21,22]. However, in many instances, it was also reported that the stress exponent determined from impression creep decreased with increasing testing temperatures, and the activation energy decreased with increasing punch stress [3,16,21–23]. For instance, activation energy values measured within a given temperature range have been observed to decrease continuously from 112 to 105 kJ/mol with increasing punch stress in Pb [22]. Likewise, experiments on  $\beta$ -Sn single crystals in [100] orientation have shown that the apparent stress exponent increases systematically from 3.6 to 4.5 with decreasing temperatures within the same stress range [21]. In some materials, such systematic temperature/stress dependency of stress exponents and activation energies truly reflect the material's creep behavior; however, as discussed subsequently, similar effects may also arise during impression

\* Corresponding author. Tel.: +1-831-656-2851;  
fax: +1-831-656-2238.

E-mail address: idutta@nps.navy.mil (I. Dutta).

62 creep due to a mechanics-induced artifact which severely  
63 prolongs the time necessary to establish steady-state creep,  
64 potentially leading to anomalous interpretations of the creep  
65 data.

66 In this paper, we discuss the source of these mechanics-  
67 induced  $\sigma_p$ - $T$  dependencies of  $Q$  and  $n$ , and prescribe a  
68 solution to minimize these effects. It will be demonstrated  
69 that these effects, while being relatively negligible in rapidly  
70 creeping materials, such as Pb [21], LiF [3], and succinonitrile  
71 [2], become quite significant in relatively slowly creep-  
72 ing materials like Sn–Ag solders under similar  $\sigma_p/G$  and  
73  $T/T_M$  conditions.

74 1.1. Finite element modeling

75 Computational simulation has been commonly employed  
76 to analyze the impression creep of different materials since  
77 analytical solutions to many impression creep problems do  
78 not exist [17,25–29]. In this study, a commercial finite ele-  
79 ment analysis (FEA) software, ANSYS<sup>TM</sup>, has been used to  
80 model the sample/punch system. which are represented in a  
81 two-dimensional (2-D) half-space of finite width (Fig. 1a)  
82 by taking advantage of the axisymmetry of the problem.  
83 The model was meshed as shown in Fig. 1b, using 667  
84 two-dimensional 8-node quadrilateral axisymmetric ele-

85 ments and 37 2-D 3-node contact elements, with a total of  
86 2068 nodes. The contact between the indenter and the spec-  
87 imen surface were modeled using contact elements with a  
88 very small coefficient of static friction ( $\mu_f = 0.0001$ ). In  
89 order to be consistent with the axisymmetry of the problem,  
90 the applied displacement boundary conditions are:

91  $u_r = 0$  along the axisymmetric axis  $A$ ,

92  $u_z = 0$  at the bottom of the specimen,

93 and

94  $u_\theta = 0$  for all the nodes.

95 Impression of the sample was simulated by applying a  
96 uniform pressure  $p_z$  on the line representing the top-surface  
97 of the punch using a built-in feature of the FEA code, such  
98 that

99  $p_z = \sigma_p$

100 where  $\sigma_p$  is the desired punch stress. In the model, the cir-  
101 cumference of the contact are the punch was assumed to  
102 have a fillet of  $0.5 \mu\text{m}$  radius, in order to avoid potential sin-  
103 gularities at the corner. It has been shown that a fillet radius  
104 of less than 5% of the indenter diameter has negligible ef-  
105 fect on the impression velocity [25], which was adopted in  
106 this study with a 1 mm diameter punch.

107 The specimen, assumed to be a 5 mm high cylinder of  
108 10 mm diameter, was modeled as an elastic–plastic-creeping  
109 solid, displaying bi-linear isotropic plastic hardening and  
110 steady-state creep via a power-law relation, given by:

111  $\dot{\epsilon} = A\sigma^n \exp\left(\frac{-Q}{RT}\right)$

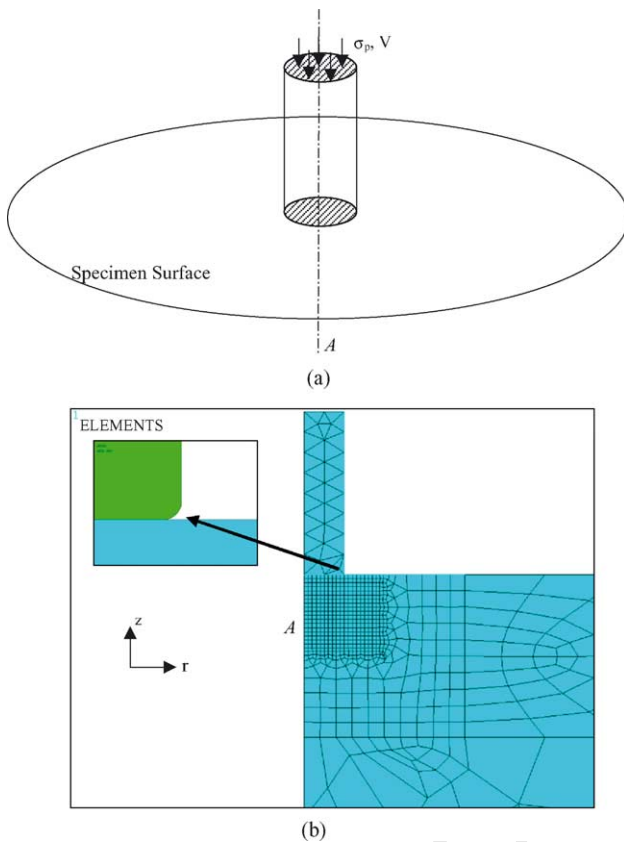


Fig. 1. (a) Schematic of impression creep of a half-plane; (b) ANSYS<sup>TM</sup> finite element mesh for the impression creep of a half-plane. A round fillet is located at the contact corner of the indenter, as shown in the inset.

Table 1  
Material properties used as input in the calculation [30,31]

Temperature (K)	Young's modulus (GPa)	Poisson's ratio
Elastic properties: material 1 (Sn–3.5Ag) [30]		
423	24.2	0.35
398	28.8	0.35
373	33.5	0.35
348	38.1	0.35
323	42.8	0.35
298	47.5	0.35
Elastic properties: material 2 (the indenter)		
All	500,000	0.2
Temperature (K)	Yield strength (MPa)	Tangent modulus (MPa)
Bilinear isotropic plastic properties: material 1 [31]		
298	30	200
373	18	184
453	10	166

Creep equation [30]:  $\dot{\epsilon} = 7.087 \times 10^{-8} (\sigma [\text{MPa}])^{5.5} \exp((-38,500 \text{ J/mol})/RT) [\text{s}^{-1}]$ .

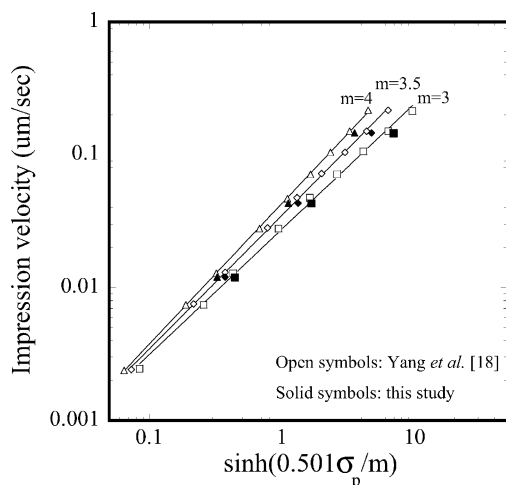


Fig. 2. Comparison shows a good agreement between the results by current FEM model and the literature results [18] for Sn–Pb eutectic alloy.

112 where  $\dot{\epsilon}$  is the creep rate;  $T$ , the absolute temperature;  $n$ , the  
 113 stress exponent;  $Q$ , the activation energy of creep;  $R$ , the uni-  
 114 versal gas constant, and  $A$ , the Dorn constant. The specimen  
 115 material chosen for the simulations is Sn–3.5Ag, a lead-free  
 116 solder of substantial current interest in the micro-electronic  
 117 packaging industry. The 1 mm diameter punch is assumed  
 118 to be non-deformable. Table 1 lists all the material constants  
 119 used in the numerical simulation.

120 After testing the model for mesh independence, its work-  
 121 ability was verified by comparing the results of impression  
 122 creep simulation on two different materials (succinonitrile  
 123 and eutectic Sn–Pb solder) with data available in the litera-  
 124 ture [2,18,25]. As shown in Fig. 2, the computed dependen-  
 125 cies of impression velocity on punch stress for the Sn–Pb  
 126 eutectic alloy displayed very good agreement with those  
 127 from the analysis of Yang et al. [25]. And for succinonitrile,  
 128 the calculated stress exponent was found to be 4.0 (Fig. 3),

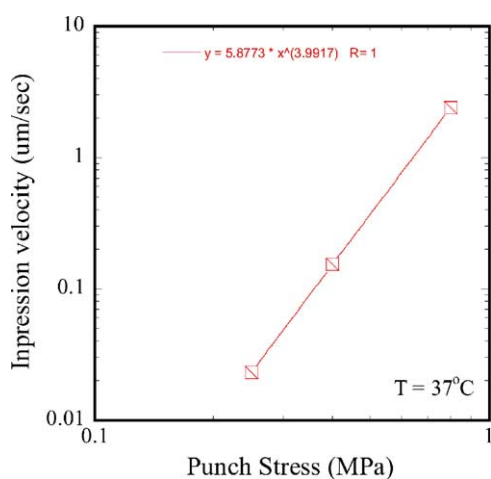


Fig. 3. The creep parameters obtained from current FEM model shows a good agreement with the input values from the literature; an example of stress exponent of succinonitrile [2] is given in this figure.

129 which is identical to the input value from the measurements  
 130 by Chu and Li [2].

131 Following model validation, the creep behavior of  
 132 Sn–3.5Ag under constant applied load was studied over a  
 133 punch stress range of 15–65 MPa and a temperature range  
 134 of 298–373 K.

## 2. Results and discussion

### 2.1. Stress and temperature dependence of creep parameters

135  
 136  
 137  
 138 A typical impression depth versus time curve is shown  
 139 in Fig. 4 and the corresponding impression velocity versus  
 140 time curve is shown in Fig. 5. Although the simulation assumed a steady-state creep law (i.e., a strain-independent constitutive creep behavior), the figures reveal the presence of a transient or primary stage, during which the impression velocity decreases gradually, eventually converging to a fixed value (i.e., a steady-state velocity) after an extended period of testing. A similar effect was noted earlier by Yu and Li [18], who suggested that the steady-state impression velocity may be deduced by polynomial extrapolation of the velocity versus reciprocal time ( $1/t$ ) data to infinite time (i.e.,  $1/t = 0$ ). However, this effect was indiscernible in experimental work on succinonitrile [2], where steady-state impression velocities were established well under 10 h for all testing conditions. In the experiments, the true primary creep region (during which the dislocation structure in the plastic zone evolves into a stable sub-structure) overlapped with, and masked the mechanics-induced transient behavior, thus enabling a steady-state impression velocity to be established within a reasonable time. It should be noted, however,

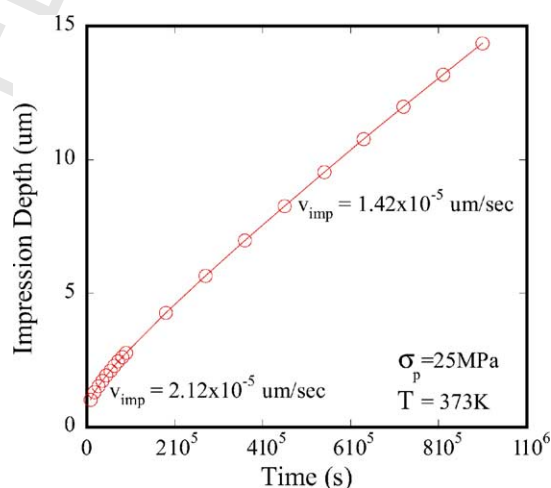


Fig. 4. Typical impression depth vs. time curve of impression creep of Sn–3.5Ag. The testing time is set to be 900,000 s (250 h) under the punch stress of 25 MPa and the testing temperature of 373 K. Note that a transient is observed even though the constitutive creep behavior is strain-independent.

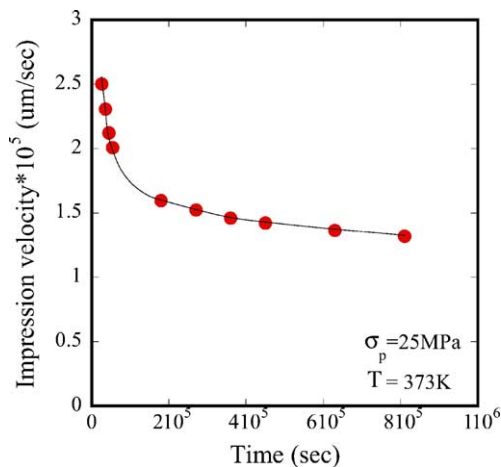


Fig. 5. The corresponding impression velocity vs. the time curve of Fig. 4. It can be seen that the impression velocity decreased with time increasing, which is consistent with the previous observations [1,18]. However, a very long time may be required to reach a 'true' steady-state.

[16]. Importantly, once the plastic zone under the punch is fully developed (i.e., when it becomes a solid hemisphere), the Von-Mises effective stress ( $\sigma_{\text{eff}}$ ) within the plastic zone remains roughly constant, as shown in Fig. 7a–c, which plot the  $\sigma_{\text{eff}}$  distributions at 90,000 s (prior to complete evolution of the plastic zone), and at 540,000 and 900,000 s (following complete evolution of the plastic zone), respectively. It is this attainment of a steady-state stress distribution within the plastic zone that produces the observed steady-state creep behavior, even though the stress state within the zone is spatially non-uniform.

Fig. 8 shows how the profile of the punch impression in the sample varies with time during a creep test. In the figure,  $x = 0$  corresponds to the punch axis. It is apparent that a distinct material pile-up appears on the sample surface around the circumference of the impression only after the plastic zone under the indenter is fully evolved (at 360,000 s or 100 h). Prior to this, the material simply slopes into the impression around the edges, without showing any significant pile-up. Thus, it may be possible to utilize the presence or absence of an edge pile-up to ascertain whether a stable stress state, and hence a steady-state, was achieved during an impression creep test, particularly under dislocation creep conditions [1], although this needs verification.

As noted above, the time required to attain a steady-state impression velocity is related to the stabilization of the stress field under the punch, which depends on the creep resistance of the testing material, the applied punch stress, and the testing temperature. For a given material, the stress field will stabilize within a shorter period under a larger punch stress and higher temperature. Under identical test conditions, materials that creep more rapidly (e.g., succinonitrile) will require less time to establish a steady impression velocity. In contrast, considerable time may elapse before the plastic zone is fully evolved (and a steady-state is reached) for a relatively slowly creeping material, e.g. Sn–3.5Ag solder.

Consequently, unless tests are conducted for very extended times to ensure that a true steady-state is reached, it is possible to infer anomalously high impression velocities. This is particularly true for tests conducted at lower stresses and temperatures, or on slowly creeping materials, where the creep rate continues to decrease very slowly even after long test times, increasing the possibility of misconstruing the strain response as having reached steady-state. If this happens, the experimentally determined  $n$  value will be temperature-dependent, while the  $Q$  value will exhibit a stress-dependence.

This is evident by comparing Figs. 9 and 10, which show plots of  $\ln V$  versus  $\ln \sigma_p$  (Figs. 9a and 10a) and  $\ln V$  versus  $1/t$  (Figs. 9b and 10b) for creep times of 90,000 s (25 h) and 900,000 s (250 h), respectively. It is clear that at 25 h, the  $n$  and  $Q$  values ( $n = 4.4$  and  $Q = 32$  kJ/mol) are significantly depressed relative to the values obtained at 250 h, which accurately reflect the input values used in the simulation ( $n = 5.5$  and  $Q = 38$  kJ/mol). This establishes two important points. First, once a true steady-state is established

that for the testing conditions used in the experimental work of [2] ( $\sigma_p \sim 0.08$ – $0.8$  MPa,  $T \sim 297$ – $327$  K), succinonitrile creeps at a strain rate of  $10^{-6}$  to  $10^{-3}$  s<sup>-1</sup>, which is two or three orders of magnitude faster than the rates expected in Sn–3.5Ag solder under the  $\sigma$ – $T$  conditions of interest ( $\sigma_p \sim 15$ – $65$  MPa,  $T \sim 298$ – $373$  K). For conditions under which the material creeps slowly, the true primary creep region may not fully mask the mechanics-induced transient behavior, thus substantially prolonging the testing time necessary to acquire steady-state data from impression creep experiments. For instance, as shown in Fig. 4, for  $\sigma_p = 25$  MPa and  $T = 373$  K, it takes approximately 360,000 s (about 100 h) for the impression velocity of Sn–3.5Ag to reach a value which is within 10% of the true steady-state velocity.

Mechanistically, this evolution of impression velocity within the transient regime may be associated with the development of the stress/strain field in the specimen immediately beneath the indenter. Fig. 6a–e show the evolution of the Von-Mises equivalent creep strain ( $\epsilon_{\text{eff}}^c$ ) within the specimen just below the punch during a creep test with  $\sigma_p = 25$  MPa and  $T = 373$  K, corresponding to the creep curve of Fig. 4. As observed in Fig. 6a, which shows the  $\epsilon_{\text{eff}}^c$  distribution after 9000 s of creep, the onset of creep occurs at the stress concentration at the corner of the indenter profile, even though the corner is filleted. With increasing time, the plastically deformed zone spreads out from the indenter corner, first becoming a hemispherical shell, and eventually evolving into a solid hemispherical shape below the punch by 360,000 s. Between 360,000 and 900,000 s, the size and shape of the plastic zone under the punch remains roughly constant, although the strain distribution inside it continues to evolve. Interestingly, the depth of the plastic zone remains roughly constant at the same order of the punch diameter throughout the entire test, in agreement with the observations of Chu and Li [2] and Dorner et al.

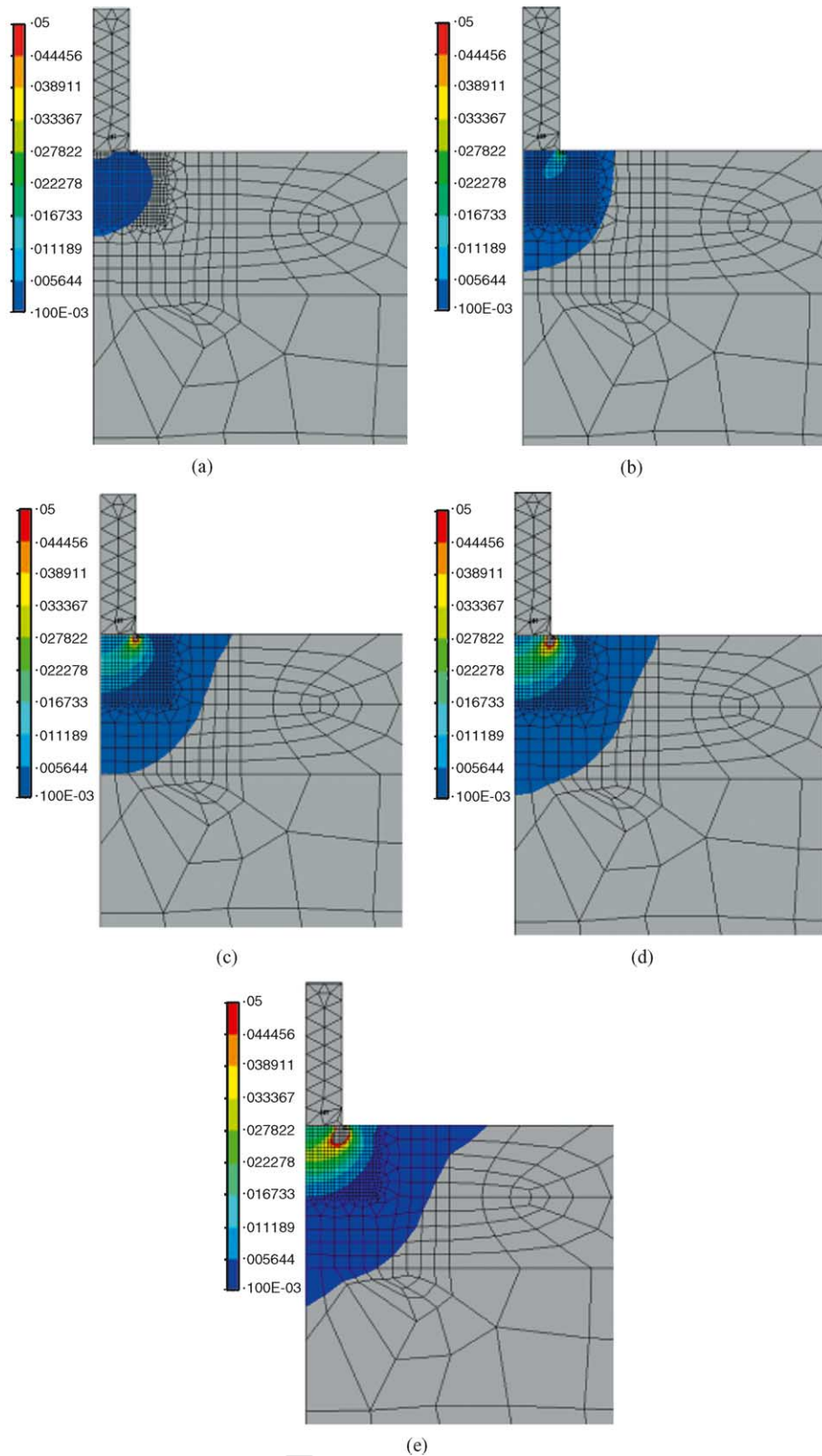
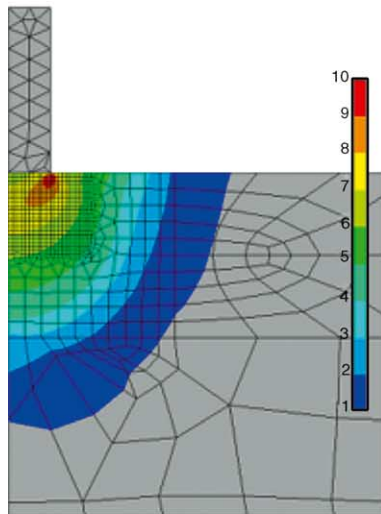
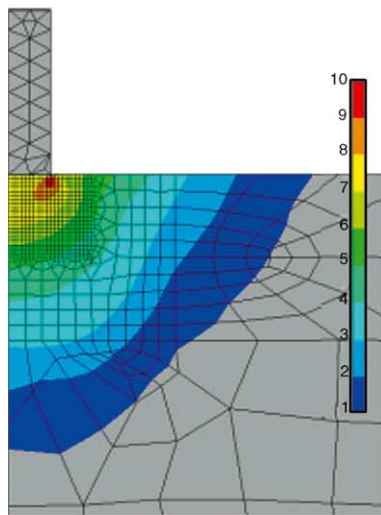


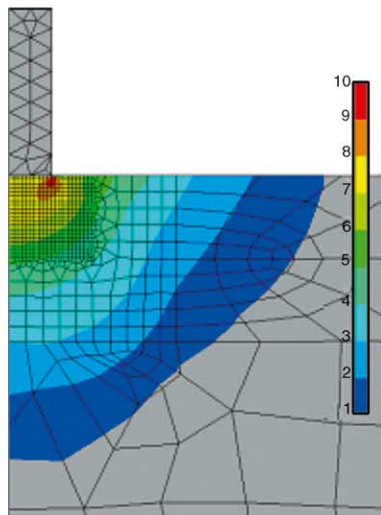
Fig. 6. The development of the strain field of an Sn–3.5Ag specimen,  $\sigma_p = 25$  MPa,  $T = 373$  K, at (a) 2.5 h (9000 s), (b) 25 h (90,000 s), (c) 100 h (360,000 s), (d) 125 h (450,000 s), and (e) 250 h (900,000 s).



(a)



(b)



(c)

Fig. 7. The development of the Von-Mises stress field of a Sn–3.5Ag specimen,  $\sigma_p = 25$  MPa,  $T = 373$  K, at (a) 25 h (90,000 s), (b) 125 h (450,000 s), and (c) 250 h (900,000 s). The unit of scale is MPa.

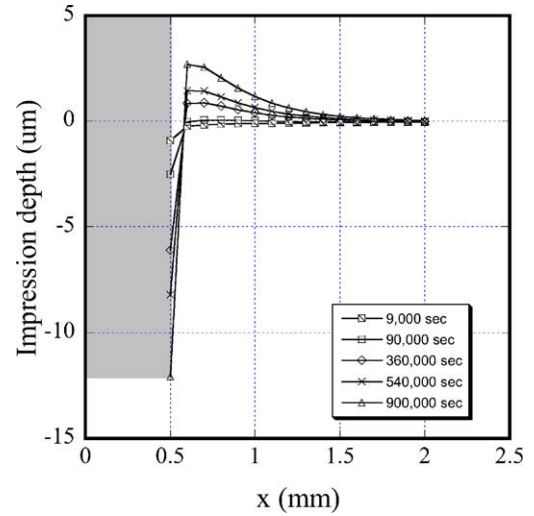
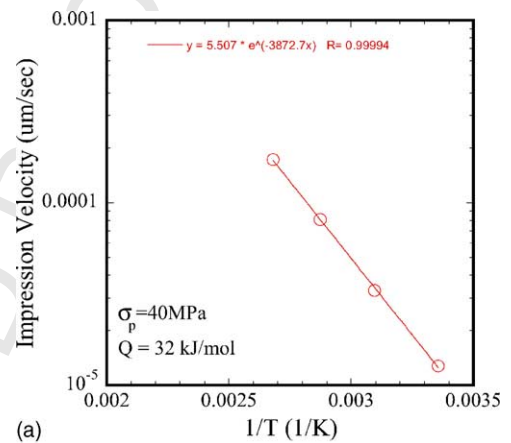


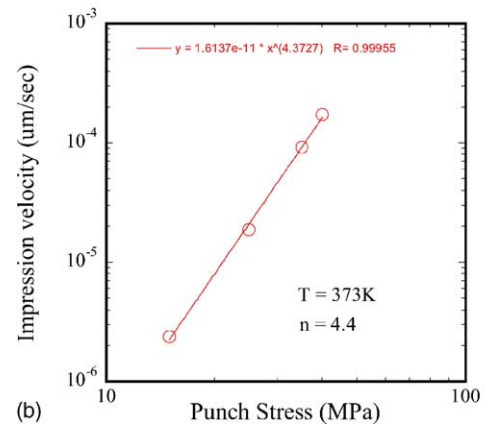
Fig. 8. The profile evolution of the sample surface with time during a test. The gray area represents the punch, and the  $x$  value indicates the distance from the punch axis.

(e.g., at 250 h), the computed creep parameters accurately reflect the true material properties. However, if sufficient care is not exercised to ensure that all the experimentally determined data points represent true steady-state behavior, the

250  
251  
252  
253

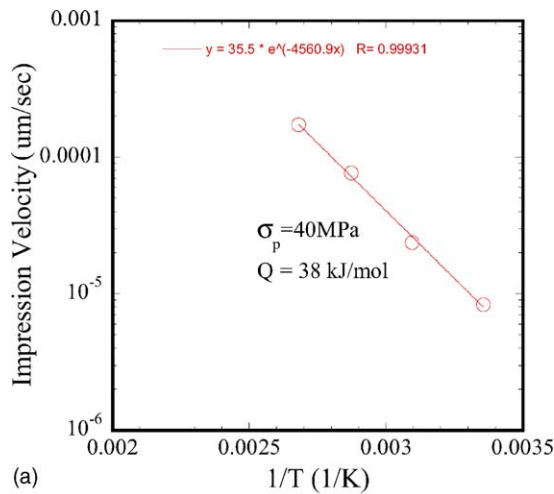


(a)

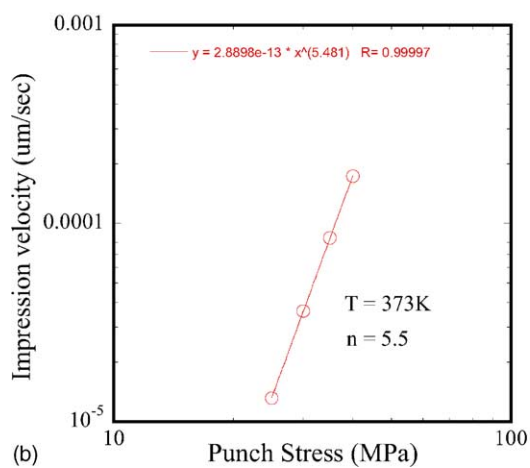


(b)

Fig. 9. The stress exponent and activation energy do not agree with the input values when the testing time is assumed to be 25 h: (a)  $Q = 32$  kJ/mol; (b)  $n = 4.4$ .

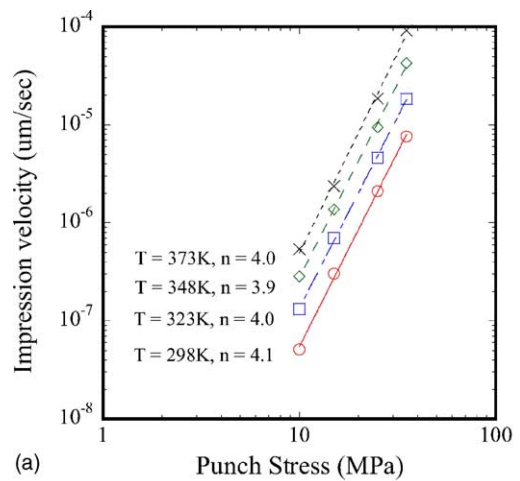


(a)

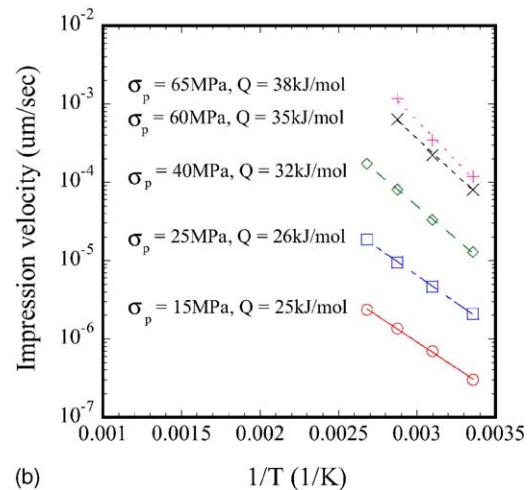


(b)

Fig. 10. The stress exponent and activation energy are identical to the input values when the testing time is assumed to be 250 h: (a)  $Q = 38$  kJ/mol; (b)  $n = 5.5$ .



(a)



(b)

Fig. 11. Illustration of stress/temperature dependencies of measured creep parameters: (a) temperature-dependent  $n$ ; (b) stress-dependent  $Q$ .

254 calculated  $n$  and  $Q$  values may be significantly depressed.  
 255 Secondly, if impression velocities from the transient regime  
 256 are used to determine the creep parameters,  $n$  values deter-  
 257 mined will exhibit temperature-dependence, whereas  $Q$  val-  
 258 ues determined will be stress-dependent. This is illustrated  
 259 in Fig. 11a and b, where the  $n$  and  $Q$  values are computed  
 260 for a range of temperatures and stresses, respectively. Sig-  
 261 nificant variations in the  $n$  and  $Q$  values are noted, depend-  
 262 ing on the conditions under which they were determined.  
 263 In general,  $Q$  values at higher  $\sigma_p$  levels are closer to the  
 264 true activation energy, since the material creep response gets  
 265 close to a true steady-state quickly under these conditions.  
 266 However, the  $n$  values determined from the transient region  
 267 appear to be constantly depressed irrespective of the test  
 268 temperatures, since at a give test temperature, the impres-  
 269 sion velocities are over-predicted at low stresses, but are  
 270 closer to the values at higher stresses. Clearly, depending  
 271 on the closeness of the various test conditions to the true  
 272 steady-state, appreciable variations of the  $n$  and  $Q$  values  
 273 may be obtained. Indeed, such stress-dependence of  $Q$  and

274 temperature-dependence of  $n$  have been observed in impres-  
 275 sion creep results [2,3,21,22], although it is unclear whether  
 276 these observations are attributable to the mechanics-induced  
 277 effect described here.

## 2.2. Proposed solution

278  
 279 It is clear from the above discussion that the mechanics-  
 280 induced transient effect may preclude accurate measure-  
 281 ment of creep parameters and produce artifacts such as  
 282 stress-dependent  $Q$  and temperature-dependent  $n$ , unless  
 283 great care is exercised to ensure that all impression velocity  
 284 data used for the computation of creep parameters repre-  
 285 sent the true steady-state. For slowly creeping materials at  
 286 low stresses and temperatures, this means that tests have to  
 287 be conducted for very long periods, eliminating one of the  
 288 primary purported advantages of impression creep, namely,  
 289 its apparent ability to establish steady-state within a short  
 290 time [1–3].

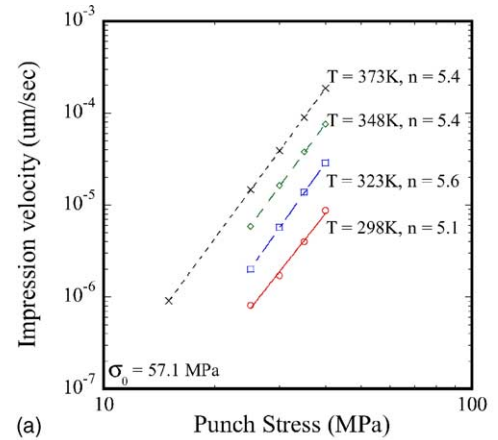
291 In the following, we seek a solution to the above problem  
 292 by developing a testing methodology to substantially accel-

293 erate the evolution of the plastic zone under the punch to a  
 294 stable state. In this methodology, the sample is plastically  
 295 impressed under a large normal stress before the creep test  
 296 is conducted, allowing a well-developed plastic zone to be  
 297 present right from the start of the creep test. As shown in the  
 298 following, this helps promote the stabilization of the stress  
 299 field within the plastic zone shortly after the beginning of  
 300 the creep test, thereby shortening the required testing time  
 301 quite substantially.

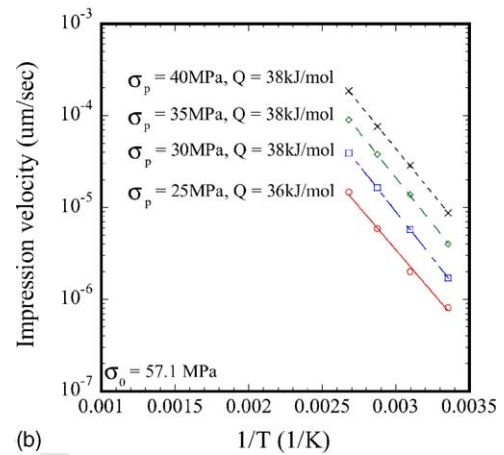
302 In the experiments simulated here by FEM, a punch stress  
 303 of 57.1 MPa was used to plastically impress the specimen  
 304 prior to creep. After the initial impression, the applied stress  
 305 was reduced to the requisite value, and the creep test was  
 306 conducted at this stress. All other conditions are the same  
 307 as those in the simulations reported above. For comparison,  
 308 a testing time of 25 h has been implemented. As depicted  
 309 in Fig. 11, the calculated  $n$  and  $Q$  values were appreciably  
 310 smaller than the input values ( $n = 5.5$ ,  $Q = 38$  kJ/mol) with-  
 311 out the presence of initial plasticity prior to the creep. How-  
 312 ever, when the creep test is preceded by an initial plastic im-  
 313 pression, the calculated  $n$  and  $Q$  show excellent agreement  
 314 with the input values, as shown in Fig. 12.

315 For comparison, typical impression depth versus time  
 316 curves, with and without the presence of initial plastic im-  
 317 pression, are presented in Fig. 13, for a punch stress of  
 318 25 MPa and temperature of 373 K during creep. It is seen that  
 319 the impression velocity with the initial plastic impression  
 320 (initial punch stress  $\sigma_0 = 57.1$  MPa) is about 40% smaller  
 321 than that without initial plasticity at 25 h and is within 10%  
 322 of the true steady-state impression velocity (as obtained af-  
 323 ter long times from the test with prior impression). Import-  
 324 antly, whereas the impression depth versus time plot without  
 325 prior plastic impression displays appreciable non-linearity  
 326 till  $\sim 56$  h, the plot is linear almost from the start when a plas-  
 327 tic impression precedes the creep test. This is attributable to  
 328 the existence of a well-defined plastic zone prior to the start  
 329 of the creep test, which allows early establishment of a stable  
 330 stress-state within the plastic zone within a short time dur-  
 331 ing the creep test. This is clear from Fig. 14a and b, which  
 332 shows the Von–Mises stress distribution in the sample after  
 333 45,000 s (12.5 h) and 90,000 s (25 h) of creep testing. It is  
 334 apparent that there is little change in the stress state within  
 335 the plastic zone during this time-range, indicating that the  
 336 prior plastic impression greatly facilitates the establishment  
 337 of a steady-state stress condition, and hence, impression ve-  
 338 locity within a short time. Thus, the proposed methodology  
 339 allows us to reduce the required test time by at least an order  
 340 of magnitude, and yet reach a true steady-state. The punch  
 341 stress required to cause the initial plastic impression must  
 342 exceed the indentation yield strength of the material, which  
 343 may be approximated as  $3\sigma_{ys}$ , where  $\sigma_{ys}$  is the uniaxial yield  
 344 strength at the appropriate temperature.

345 In addition to enabling the establishment of a true  
 346 steady-state within much shorter test times, the initial plastic  
 347 impression also serves a practical purpose related to the test  
 348 procedure. Our experimental work has shown that it is very



(a)



(b)

Fig. 12. With the aid of initial plastic impression, a significant reduction of testing time is achieved and the true creep parameters are obtained under a wide range of  $\sigma_p$  and  $T$  conditions after only 25 h (90,000 s) of testing: (a) stress exponent; (b) activation energy.

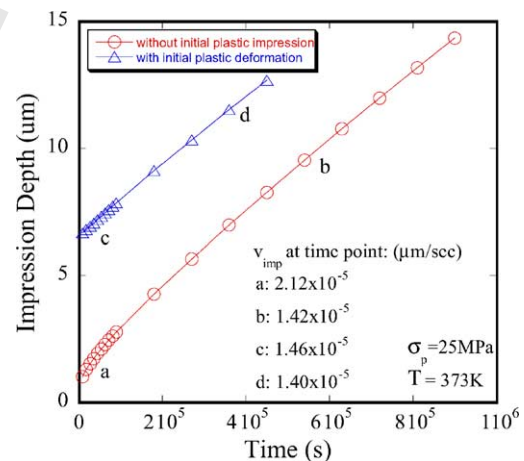


Fig. 13. Typical impression depth vs. time curves with and without the presence of initial plastic impression,  $\sigma_p = 25$  MPa,  $T = 373$  K. The slopes associated with different regions of the two plots are also noted. It can be seen that the required testing time is much shorter to reach the true steady-state creep by introduction of the initial plastic impression.

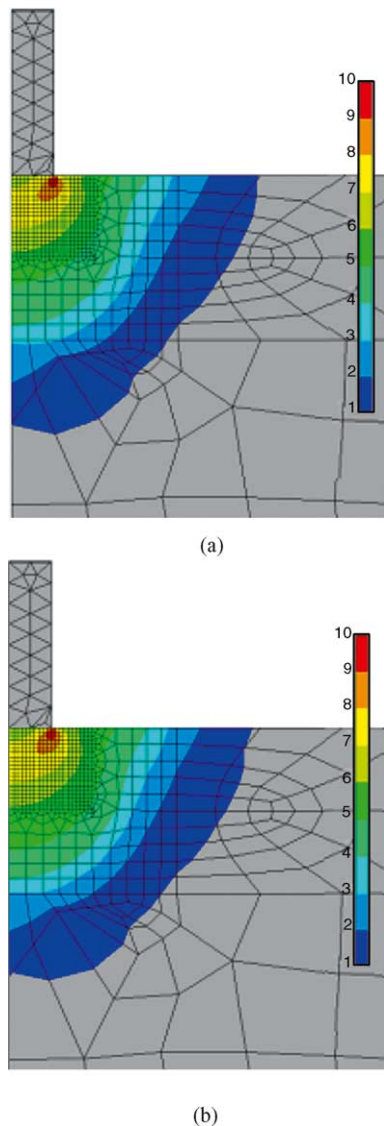


Fig. 14. The development of the Von–Mises stress field of a Sn–3.5Ag specimen,  $\sigma_p = 25$  MPa,  $T = 373$  K at (a) 12.5 h (45,000 s) and (b) 25 h (90,000 s). It is seen that after initial plastic impression the creep reaches the steady-state within a much shorter time. The unit of scales is MPa.

349 difficult to align the indenter axis exactly perpendicularly to  
 350 the specimen surface, even when considerable care is exer-  
 351 cised in mounting the punch and sample, and a self-leveling  
 352 specimen stage with a universal ball joint is utilized [32].  
 353 This is evidenced by frequent observation of gibbous impres-  
 354 sions following creep testing, suggesting that the entire  
 355 punch-tip did not come in contact with the sample even after  
 356 long test times. For instance, when the axis of an indenter of  
 357 diameter  $D$  deviates from the normal to the sample surface  
 358 by an angle  $\theta$ , a punch penetration of  $D \sin \theta$  is necessary  
 359 before the entire punch face comes in contact with the  
 360 sample. For  $\theta = 1^\circ$ , and  $D = 1$  mm, this amounts to an im-  
 361 pression depth of  $17.5 \mu\text{m}$ . While typical impression depths  
 362 much greater than this are readily obtained even under low

stress/temperature conditions for rapidly creeping materials 363  
 like Pb, succinonitrile, or even pure Sn [2,21,22], in slowly 364  
 creeping materials like Sn–3.5Ag solder, the impression 365  
 depths are often much smaller, even after testing for 8–10 h. 366  
 In this case, the indenter face never fully contacts the sam- 367  
 ple surface, allowing the effective punch stress to gradually 368  
 decrease as indenter-sample contact area increases with in- 369  
 creasing impression depth. This precludes the establishment 370  
 of a true steady-state, and thus leads to anomalous results. 371  
 However, when the sample is plastically impressed prior to 372  
 creep, this problem completely eliminated, since the plastic 373  
 impression ensures that entire punch tip is in contact with 374  
 the sample right from the start of the creep test. 375

One concern that arises when a prior plastic impression is 376  
 utilized is that it is tantamount to a stress-decrease creep test, 377  
 since the test stress is typically lower than the stress used 378  
 for the initial impression. This requires that a steady-state 379  
 dislocation structure corresponding to the test stress and 380  
 temperature conditions be established under the punch be- 381  
 fore meaningful creep data can be obtained from the test. 382  
 Since the initial plastic impression would result in a plastic 383  
 zone with much higher dislocation density than what would 384  
 be produced by the test stress, this structure has to recover 385  
 to a structure representative of the test conditions before a 386  
 steady-state behavior is obtained, potentially prolonging the 387  
 primary stage significantly. However, our experiments show 388  
 that this recovery occurs quite readily, with little obvious 389  
 prolongation of the primary stage, even under conditions of 390  
 low stress and temperature [32]. It is likely that the addi- 391  
 tional recovery time required when a prior plastic impres- 392  
 sion is used is more than compensated by the smaller time 393  
 necessary to (1) establish full contact between punch and 394  
 sample, and (2) overcome the mechanics-induced transient 395  
 effect. Thus, the approach proposed here proffers an effec- 396  
 tive means to enhance the accuracy of impression creep re- 397  
 sults by reducing artifacts arising from the mechanics of the 398  
 test, and the test set-up. The proposed solution is particularly 399  
 beneficial for slowly creeping materials such as Sn–3.5Ag 400  
 solders, where these artifacts can be particularly debilitating. 401

### 3. Conclusion 402

A mechanics-induced artifact, which can lead to anoma- 403  
 lous interpretation of impression creep data, has been iden- 404  
 tified. This effect causes the appearance of an extended 405  
 transient regime in the creep curve, even when the con- 406  
 stitutive creep behavior is strain-rate independent. It has 407  
 been shown that this mechanics-induced transient regime 408  
 coincides with the time-period over which the plastic zone 409  
 under the impression punch grows and evolves to a stable 410  
 shape corresponding to a solid hemispherical cap. Once 411  
 the plastic zone attains this shape, the Von–Mises stress 412  
 distribution inside the zone becomes stable, and does not 413  
 change appreciably with ongoing creep. This results in a 414  
 true steady-state impression velocity, and creep parameter 415

(i.e.,  $n$  and  $Q$ ) calculations using this steady-state velocity accurately reflect material properties. However, very prolonged test times may be necessary to establish this true steady-state behavior, particularly for slowly creeping materials and/or low stress-temperature conditions. In order to rapidly establish true steady-state behavior, and minimize the possibility of erroneous creep parameter computations, an experimental methodology is proposed to substantially shorten the requisite test time. This involves plastically impressing the sample surface prior to creep testing, in order to facilitate the development of the plastic zone under the punch. It is shown that this procedure also yields accurate creep parameter computations, but based on substantially shorter tests than in the absence of a prior plastic impression.

#### 430 Uncited references

431 [24,33].

#### 432 Acknowledgements

433 This work is supported by an NSF-GOALI program  
434 in partnership with INTEL Corporation (grant # DMR-  
435 0209464) and SRC contract # 2002-NJ-1004. The collabo-  
436 ration and mentorship of Dr. R. Mahajan and Mr. S. Jadhav  
437 of INTEL are gratefully acknowledged.

#### 438 References

- 439 [1] J.C.M. Li, Mater. Sci. Eng. A322 (2002) 23.  
440 [2] S.N.G. Chu, J.C.M. Li, J. Mater. Sci. 12 (1977) 2200.  
441 [3] E.C. Yu, J.C.M. Li, Phil. Mag. 36 (1977) 811.  
442 [4] H.Y. Yu, M.A. Imam, B.B. Rath, in: Proceedings of the Fifth Inter-  
443 national Conference on Ti, vol. 3, Munich, 1983, p. 1819.  
[5] C.P. Pang, H.Y. Yu, J. Chung Cheng Inst. Tech. 14 (1984) 111.

- [6] M. Yamaguchi, Y. Umakoshi, T. Yamane, Trans. Iron Steel Inst. Jpn. 444  
25 (1985) B367–B367. 445  
[7] P.S. Godavarti, S. Hussien, K.L. Murty, Metall. Trans. 19A (1988) 446  
1243. 447  
[8] N.Q. Chinh, Z.S. Rajkovits, G. Voros, I. Kovacs, Key Eng. Mater. 448  
44/45 (1990) 257. 449  
[9] P. Gondi, A. Sili, Z. Metallkunde 82 (1991) 377. 450  
[10] K.L. Murty, Met. Forum 15 (1991) 217. 451  
[11] V. Raman, R. Berriche, J. Mater. Res. 7 (1992) 627. 452  
[12] T.H. Hyde, K.A. Yehia, A.A. Becker, Mater. High Temp. 13 (1995) 453  
133. 454  
[13] P.P. Rao, K.S. Swamy, Z. Metallkunde 86 (1995) 760. 455  
[14] F. Yang, J.C.M. Li, Mater. Sci. Eng. A201 (1995) 40. 456  
[15] R.S. Sundar, T.R.G. Kutty, D.H. Sastry, Intermetallics 8 (2000) 427. 457  
[16] D. Dorner, K. Roller, B. Skrotzki, B. Stockhert, G. Eggeler, Mat. 458  
Sci. Eng. A, in press. 459  
[17] F. Yang, J. Chen, I. Seidmann, J.C.M. Li, Mater. Sci. Eng. A207 460  
(1996) 30. 461  
[18] H.Y. Yu, J.C.M. Li, J. Mater. Sci. 12 (1977) 2214. 462  
[19] P.S. Godavarti, K.L. Murty, J. Mater. Sci. Lett. 6 (1987) 456. 463  
[20] A.A. Becker, T.H. Hyde, L. Xia, J. Strain Anal. Eng. Des. 29 (1994) 464  
185. 465  
[21] S.N.G. Chu, J.C.M. Li, Mater. Sci. Eng. 39 (1979) 1. 466  
[22] D. Chiang, J.C.M. Li, J. Mater. Res. 9 (4) (1994) 903. 467  
[23] N.Q. Chinh, P. Tasnadi, A. Juhasz, P. Szommer, E. Szep-Kiss, I. 468  
Kovacs, Key Eng. Mater. 97/98 (1994) 159. 469  
[24] P. Yavari, T.G. Langdon, Acta Metall. 30 (1982) 2181. 470  
[25] F. Yang, J.C.M. Li, C.W. Shih, Mater. Sci. Eng. A201 (1995) 50. 471  
[26] T.H. Hyde, K.A. Yehia, A.A. Becker, Int. J. Mech. Sci. 35 (1993) 472  
451. 473  
[27] B. Storakers, P.-L. Larsson, Royal Institute of Technology Report 474  
154, Royal Institute of Technology, Stockholm, 1992. 475  
[28] Z.F. Yue, G. Eggeler, B. Stockhert, Comput. Mater. Sci. 21 (2001) 476  
37. 477  
[29] Z.F. Yue, M. Probst-Hein, G. Eggeler, Mater. High Temp. 17 (4) 478  
(2000) 449. 479  
[30] B. Storakers, P.L. Larsson, J. Mech. Phys. Sol. 42 (1994) 307. 480  
[31] R. Darveaux, K. Banerji, IEEE Trans. Components Hybrids Manuf. 481  
Technol. 15 (6) (1992) 1013. 482  
[32] J.-K. Lin, A.D. Silva, D. Frear, Y. Guo, S. Hayes, J.-W. Jang, L. Li, 483  
D. Mitchell, B. Yeung, C. Zhang, IEEE Trans. Electron. Packaging 484  
Manuf. 25 (3) (2002) 300. 485  
[33] I. Dutta, C. Park, S. Choi, in: Proceedings of InterPack 2003, ASME 486  
2003, in press. 487